Bridge Scour in Lakes due to Waves

Tehseena Ali,[1] Jean-Louis Briaud,[2] and Hamn-Ching Chen[3]

[1]Zachry Department of Civil and Environmental Engineering, Texas A&M University, P.O. Box 3136, College Station, TX 77843-3136, USA; e-mail: rumeeameen@tamu.edu Corresponding author.
[2]Zachry Department of Civil and Environmental Engineering, Texas A&M University, P.O. Box 3136, College Station, TX 77843-3136, USA; e-mail: briaud@tamu.edu
[3]Zachry Department of Civil and Environmental Engineering, Texas A&M University, P.O. Box 3136, College Station, TX 77843-3136, USA; e-mail: hcchen@civil.tamu.edu

ABSTRACT

Waves generated by the wind blowing over a water surface are prevalent in most marine and lacustrine environments. They may be the primary driver of erosion in these environments, causing bridge scour. According to a survey conducted in this project, there is no guidance to perform scour evaluation for bridges in lakes and reservoirs (shallow water), leading to several bridges being out of compliance with the national inspection standards. The methodology to determine scour depth in shallow waters presented in this article was developed by assembling existing components collected after an extensive literature review. The proposed procedure regroups elements of existing research into a step-by-step approach, allowing the engineer to predict scour around bridge support in lakes. It involves the calculation of key parameters such as significant wave height, peak wake period, bottom orbital velocity, and the collection of other parameters including water depth, pier diameter, fetch, and wind speed. Three bridges in Texas were selected as subjects of the study and used for a parametric study. The results indicate that the maximum scour depth in shallow waters averages one-half of the pier diameter and decreases with an increase in water depth while increasing with an increase in pier diameter, fetch, and design wind speed.

INTRODUCTION

Most of the scour research conducted since late 1980 has been focused on developing appropriate methodologies and formulas for scour depth estimation around the foundation of riverine or coastal bridges. However, little research has thus far focused on bridges spanning lakes and reservoirs susceptible to scour. Winds are one of the prominent factors initiating the horizontal motion of water in lacustrine systems, and waves generated by the wind blowing over the water surface are prevalent in most marine and lacustrine environments. In lacustrine and similar environments, soil erosion around bridge foundations is influenced by wind-generated waves, as described by various researchers (Olsen, 2002; Sumer et al., 2007). Many guidance documents (e.g., HEC 18) for soil erosion and scour at bridge supports are available; though comprehensive, they do not cover the

case of wave scour in a lacustrine environment. Other documents like HEC 25 have excellent coverage of coastal processes, including waves but little guidance on wave scour. The survey conducted in the United States shows that most of the DOTs (Department of Transportations) do not have any design for wave-induced scour analysis and thus do not identify any separate guidance document for bridges in lakes/reservoirs, leading to several bridges out of compliance from the national inspection standard. This article introduces a novel approach for determining the scour depth around bridge supports in shallow waters. The proposed methodology synthesizes and organizes various components of previous research into a step-by-step procedure that can be utilized to accurately predict the extent of scour around bridge piers in lakes.

WAVE PARAMETER PREDICTION IN SHALLOW WATERS

Wave heights and periods vary across the fetch length due to the energy the wind transfers to the water's surface. Phillips developed the resonance model (Phillips, 1957) to explain wave behavior by studying the interaction between wind and water. Meanwhile, the shear flow model (Miles, 1957) describes how the wind velocity changes with height, resulting in differences in wind stress on the water's surface, which affects the currents and wave formation. A new theory (Longuet-Higgins, 1969) was devised to explain how energy is transferred between the wind and the waves. Longer waves break on the crests of lesser waves that are going more quickly as the wave heights rise. Consequently, wave period and height rise when fetch, wind speed, or duration rises.

The wave properties in a fetch-limited situation are determined only by the fetch length and wind speed, assuming steady-state conditions are reached. If the wind speed is too low, it becomes duration-limited, which is rarely observed. There is a maximum fetch length, beyond which waves will not continue to grow even if the wind blows indefinitely, resulting in a fully formed sea where energy input is balanced with dissipation through wave breaking and turbulence (Sorensen, 1993).

Compared to a thorough numerical approach, forecasting growth curves allows one to estimate wave properties more quickly while offering reasonably accurate numbers. It is commonly acknowledged that the SMB (Sverdrup-Munk-Bretschneider) method (SPM, 1973) is the most practical and reliable technique for computing wave heights and durations in deep water when limited time and data are available.

Currently, various numerical models are available for forecasting wave fields in areas with complex wind and bathymetric environments. The third-generation spectral model (SWAN) developed by The Technical University of Delft (Ris et al., 1999) is commonly used in coastal engineering and science. Another third-generation wave analysis model called WAM was developed, which utilizes the concept of a wind-wave energy spectrum to solve balancing equations on a global scale (Lin et al., 2002). The current effort for predicting wave characteristics will, however, be limited to a comparatively straightforward semi-empirical model depending on wind conditions since it is meant to be used by field practitioners.

The SPM recommends a parametric model for forecasting wave characteristics in shallow waters (SPM, 1984). The Coastal Engineering Manual which is an improved version of SPM presents a modified approach for predicting waves due to wind (Vincent et al., 2002). The SPM approach computes T_p (peak period: time interval between successive wave crests (or troughs) of the most energetic waves in a wave group) and H_s (significant wave height: the average height of the highest one-third of waves in a given sea state) based on energy, using the inputs of duration, fetch, and wind speed, which can be written as:

$$H_s, T_p = f(U_A, F, t_d, d_w) \tag{1}$$

where U_A is called the wind stress factor, F is the fetch length, t_d is the duration of the wind, and d_w is the water depth. The rate at which momentum from the wind is transferred to the waves is represented by the wind stress factor, which is given by:

$$U_A = 0.71\, U_{10}^{1.23} \tag{2}$$

where U_{10} denotes the average speed of wind at an elevation of 10 m above the mean level of water and is expressed as:

$$U_{10} = U_z \left(\frac{10}{z}\right)^{1/7} \tag{3}$$

where U_z is the speed of wind at a height z. To predict wave parameters accurately, it is necessary to have information about the wind speed in the vicinity of the water surface for a suitable period of time. The time interval considered should ideally be equivalent to the duration required for waves to traverse the distance of the available fetch, which permits the assumption of fetch-limited conditions.

Dimensional analysis of the basic wave generation relationship yields (Hughes, 1993):

$$\frac{gH_s}{{U_A}^2}, \frac{gT_p}{U_A} = f\left(\frac{gF}{{U_A}^2}, \frac{gt_d}{U_A}, \frac{gh_w}{{U_A}^2}\right) \tag{4}$$

The required time for waves to traverse the length of fetch is called t_{min} (minimum duration) and winds are referred to as duration-limited if the duration of the wind is shorter than t_{min}. However, if the wind persists for a duration that exceeds t_{min}, the waves are fetch-limited. In this scenario, the wave parameters become independent of the ratio gt_d/U_A, provided the wind is sustained enough in both direction and intensity to maintain fetch-limited conditions. For the fetch-limited condition, Equation 4 is simplified to:

$$\frac{gH_s}{{U_A}^2}, \frac{gT_p}{U_A} = f\left(\frac{gF}{{U_A}^2}, \frac{gh_w}{{U_A}^2}\right) \tag{5}$$

The relationship described in Equation 5 indicates that H_s and T_p are dependent on the speed of the wind, the length of fetch, and the depth of water. To predict waves in shallow water based on wind characteristics, SPM provides the following parametric model:

$$H_s = \frac{U_A^2}{g} \times 0.283\ tanh\left[0.530\left(\frac{gd_w}{U_A^2}\right)^{3/4}\right] tanh\left\{\frac{0.00565\left(\frac{gF}{U_A^2}\right)^{1/2}}{tanh\left[0.530\left(\frac{gd_w}{U_A^2}\right)^{3/4}\right]}\right\} \tag{6}$$

$$T_p = \frac{U_A}{g} \times 7.54\ tanh\left[0.833\left(\frac{gd_w}{U_A^2}\right)^{3/8}\right] tanh\left\{\frac{0.0379\left(\frac{gF}{U_A^2}\right)^{1/3}}{tanh\left[0.833\left(\frac{gd_w}{U_A^2}\right)^{3/8}\right]}\right\} \quad (7)$$

where g is the acceleration due to gravity, H_s is the significant wave height, d_w is the depth of water, F is the fetch and T_p is the peak period.

BOTTOM ORBITAL VELOCITY

Wind-induced waves create circular motion in the water column, known as orbital motion, which extends to a depth of about half the wavelength of surface waves. This orbital motion decreases exponentially with the water depth, and the water beyond half of the wavelength is essentially unaffected by the wave action. This indicates that wave scour will mostly occur in shallow waters and likely near the shore. Shallow water waves emerge when the water depth is less than 1/20 of the wavelength. In the case of shallow and intermediate depths, the wave orbital velocity can reach the seafloor or lake bottom (Figure 1a) with little or no decay. In deep-water waves (Figure 1b), the orbital motion is circular and decreases with depth, and at a depth of about one-half of the wavelength, this orbital motion becomes small.

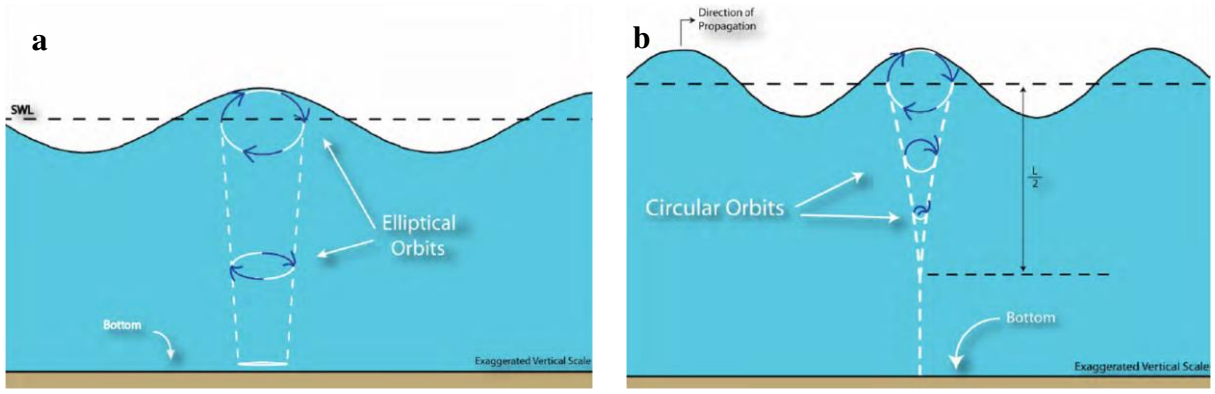

Figure 1. (a) Orbital velocity in shallow and intermediate water, (b) Orbital velocity in deep water. (Douglass & Krolak, 2008).

Theoretical models describe water flow near the bed for low-amplitude, monochromatic waves. Madsen (Madsen, 1994) extended these models to a wave spectrum if known, but estimating orbital velocities is challenging when only summary statistical parameters like H_s and T_p are available. A solution is to use a generic spectral form, such as Soulsby's method (1987), to approximate the contribution of the entire wave spectrum to bed flow by combining these parameters.

The interaction between surface waves and the seabed is typically described by the wave-induced fluid motion close to the bed. The most straightforward way to express this motion is through the horizontal component of the wave-induced orbital velocity (u_0), evaluated at the bottom ($z = d_w$), as predicted by linear wave theory for small amplitude, monochromatic waves.

$$u_0 = \frac{H\pi}{Tsinh(kd_w)} cos(kx - \omega t) \quad (8)$$

where H is the wave height, T the wave period, d_w the water depth, k the wavenumber (equal to $2\pi/L$), L is the wavelength, ω is the circular frequency (equal to $2\pi/T$), x is the coordinate in the direction of wave propagation, and t is the time. As z approaches d_w, the vertical component of the orbital velocity approaches zero. The horizontal component of the orbital velocity, u_0, varies sinusoidally over a wave period, reaching a maximum velocity, which is commonly known as the bottom orbital velocity u_m, when $|cos(kx - \omega t)| = 1$:

$$u_m = \frac{H\pi}{Tsinh(kd_w)} \quad (9)$$

Equation 9 states that the bottom orbital velocity is directly proportional to the wave height and inversely proportional to the water depth. The relationship between bottom orbital velocity (u_m) and wave period is more complicated because the wave period affects the equation through both k and T. The value of k is defined as $4\pi^2/[gT^2 tanh(kd_w)]$, and the term $Tsinh(kd_w)$ decreases as the wave period increases. Consequently, longer-period waves produce larger bottom orbital velocities. The effect of increasing wave period on u_m becomes more pronounced as the water depth increases. The differences are smaller in shallow water because orbital velocities are primarily a function of depth $\left(u_m = a\sqrt{g/d_w}\right)$ when $sinh(kd_w)$ is approximately equal to kd_w.

Wave properties are commonly described by significant wave height and peak wave period. Natural waves exhibit a range of frequencies, amplitudes, and directions. When only significant wave height and zero-crossing period are known, a two-parameter spectrum like JONSWAP (Joint North Sea Wave Project) can estimate the surface elevation spectrum (Hasselmann, 1973). Other empirical wave spectra are also available, but their applicability depends on specific oceanic conditions. These spectra can be written in the following general form:

$$S_n(f) = \frac{\alpha g^2}{(2\pi)^4 f^5} \left(\frac{f}{f_p}\right)^{\xi} \times exp\left[-\beta \left(\frac{f}{f_p}\right)^{-4}\right] \gamma^{exp\left[-(f-f_p)^2/(2\sigma^2 f_p^2)\right]} \quad (10)$$

The JONSWAP spectrum is characterized by f_p (peak frequency $\left(= 1/T_p\right)$) and parameters such as α, β, ξ, γ and σ that control its magnitude and shape. These parameters can be constants or functions of the ratio of frequency to peak frequency (f/f_p) or external variables such as fetch length and mean wind speed. Using curve fitting techniques, an equation for the root-mean-squared velocity (u_m) of the wave can be obtained from the JONSWAP spectrum. This equation was derived by Soulsby (1987) and provides an explicit algebraic expression for u_m as follows:

$$u_m = \frac{0.25}{(1+At^2)^3} \times \frac{H_s}{T_n} \quad (11)$$

where $A = [6500 + (0.56 + 15.54t)^6]^{1/6}$, $t = T_n/T_z$, H_s is the significant wavelength, T_n is a natural scaling period $\left[= (d_w/g)^{1/2}\right]$ and T_z is the zero-crossing period $\left[= \left(T_p/1.281\right)\right]$.

WAVE INDUCED SCOUR

In lacustrine and similar environments, soil erosion around bridge foundations is influenced by wind-generated waves, as described by various researchers (Olsen, 2002; Sumer et al., 2007). These waves produce orbital velocities that reach the bed and dissipate as they interact with the sediment, generating shear stresses that can exceed the critical shear stress of the soil. As a result, soil particles can become suspended in the flow or displaced on the lakebed, leading to the erosion of sediment around the bridge foundation (Gazi et al., 2019). When a bridge pier is placed in a lake or other similar environment, the flow of water around the pier is affected by several factors, including the narrowing of the flow path, the formation of a horseshoe-shaped vortex in front of the pier, and the creation of swirling patterns behind the pier known as lee-wake vortices, which may or may not lead to the shedding of vortices. The mechanism of scour in waves is described by Sumer et al. (2007). These vortices can increase the capacity of sediment transport locally and can lead to the erosion of sediment around the pier, which threatens its stability. Researchers have observed that under certain flow conditions, sediment is picked up from the bed and moved to the core of the lee-wake vortex, eventually shedding as a separate vortex. This leads to significant erosion around the pier.

The dynamics of wave-induced scour are influenced primarily by two factors: the Keulegan-Carpenter number (KC number) and the diffraction parameter (d_p/L) (Dey et al., 2006; Sumer et al., 2007; Webb and Matthews, 2014; Gazi et al., 2019). The diffraction parameter is the ratio of the diameter of the bridge pier (d_p) to the wavelength of the waves (L), while the KC number is the ratio of the length of the flow to the length of the structure, and is expressed as:

$$KC = \frac{u_m T_p}{d_p} \tag{12}$$

where u_m is the bottom orbital velocity, T_p is the peak period and d_p is the diameter of the bridge pier. KC number plays a crucial role in determining the extent of scouring near the bridge foundation. The KC number indicates the balance between the flow and structure length. A KC number less than 1 suggests that the scouring process is started by steady flow in the lower layer, whereas a KC number greater than 1 indicates the existence of downflow upstream of the foundation because of the pressure gradient. If the KC number exceeds 6, lee-wake vortices can be created due to flow disturbance (Webb and Matthews, 2014).

The normalized equilibrium scour depth (NESD) (Sumer & Fredsøe, 1998) represents the functional relationship between scour depth (S) and pile diameter (d_p). This relationship is established according to several factors, including sediment number, Shields' parameter, pile Reynolds number, and KC number as follows:

$$\frac{S}{d_p} \sim f\left(\frac{u_m}{\sqrt{g(s-1)d_{50}}}, \frac{u_{fm}^2}{g(s-1)d_{50}}, \frac{u_m d_p}{v}, \frac{u_m T_p}{d_p}\right) \tag{13}$$

where g is the acceleration due to gravity, v is the kinematic viscosity, s is the specific gravity of solids, d_{50} is the median sediment diameter, u_m is the maximum orbital velocity, u_m^f is the maximum frictional velocity, and T_p is the peak period. Research has shown that the KC number is the main factor that determines the equilibrium scour depth on a live bed. Figure 3 (Webb &

Matthews, 2014) shows a comparison of the measured maximum normalized equilibrium scour depth (NESD) as a function of KC for waves and cylindrical piles over a KC number range of $0.1 < KC < \infty$.

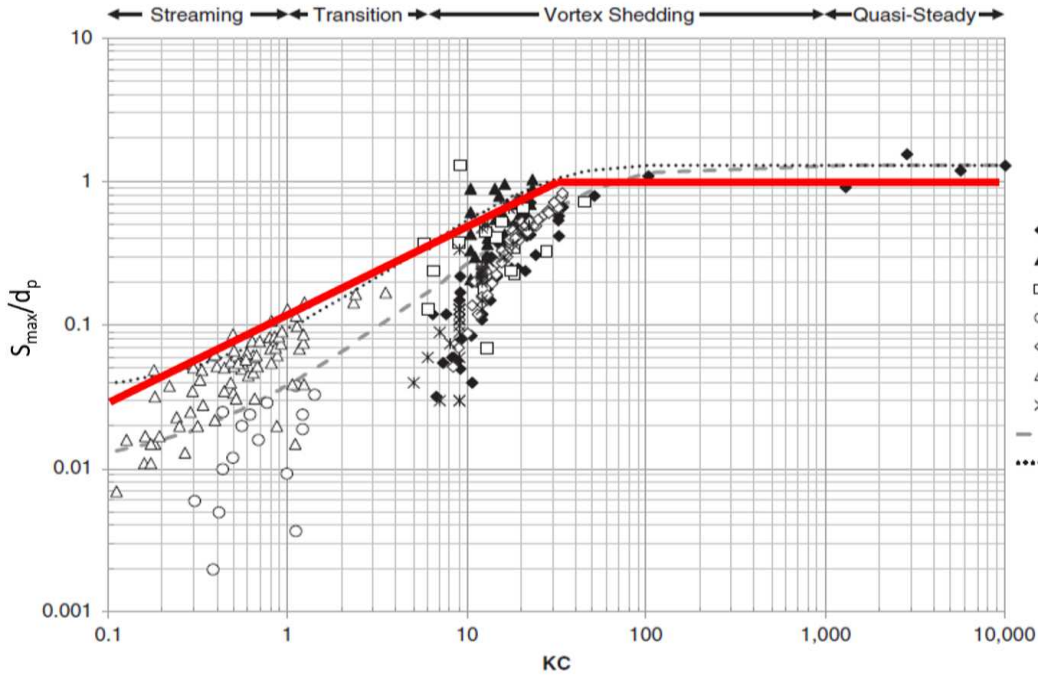

Figure 3. Comparison of maximum Normalized Equilibrium Scour Depth (NESD) as a function of KC for wave scour around cylindrical piles (Webb & Matthews, 2014).

STEP-BY-STEP PROCEDURE

After conducting an extensive review of the relevant literature, a methodology to determine the scour depth in the case of shallow water was developed for wave scour. This methodology consists of a series of steps including data collection and data analysis. The input parameters required for different steps are commonly available and easily obtainable through standard data collection methods or existing sources. A step-by-step procedure is as follows:

1. Select the design wind speed (U_w): The 100-year wind speed at the site where the structure is located may be selected as a typical design wind speed. Obtain historical wind data from reliable sources e.g., meteorological stations, airports, or other sources that collect weather data. If the winds are not measured at the 10-meter elevation, the windspeed must be adjusted accordingly by the following equation:

$$U_{10} = U_z \left(\frac{10}{z}\right)^{1/7}$$

where, U_{10} is the wind speed at 10 m elevation, U_z is the measured wind speed at some elevation, z is the elevation. Using wind frequency analysis and a chosen probability

distribution, a 100-year wind speed can be obtained (Briaud et al., 2023). The 100-year wind speed is essential because it is used to estimate the design wave height and period for the structure.

2. Determine significant wave height (H_s) and peak period (T_p) of the design wave: This can be done using a variety of methods, including empirical formulas, numerical methods, or by analyzing historical wave data. The expressions referenced above for shallow water (Equation 6 and Equation 7) are recommended to calculate H_s and T_p. Shallow water conditions are assumed for this procedure and the expressions are not suitable for deep water conditions.

$$H_s = \frac{U_A^2}{g} \times 0.283\ tanh\left[0.530\left(\frac{gd_w}{U_A^2}\right)^{3/4}\right] tanh\left\{\frac{0.00565\left(\frac{gF}{U_A^2}\right)^{1/2}}{tanh\left[0.530\left(\frac{gd_w}{U_A^2}\right)^{3/4}\right]}\right\}$$

$$T_p = \frac{U_A}{g} \times 7.54\ tanh\left[0.833\left(\frac{gd_w}{U_A^2}\right)^{3/8}\right] tanh\left\{\frac{0.0379\left(\frac{gF}{U_A^2}\right)^{1/3}}{tanh\left[0.833\left(\frac{gd_w}{U_A^2}\right)^{3/8}\right]}\right\}$$

where g is the acceleration due to gravity, H_s is the significant wave height, d_w is the depth of water, F is the fetch, T_p is the peak period, d_w is the depth of water, and U_A is the wind stress factor.

3. Check water depth against wavelength: The wavelength is calculated using the following equation:

$$L = \frac{gT_p^2}{2\pi} tanh\left(\frac{2\pi d_w}{L}\right) \quad (14)$$

where L is the wavelength, g is the acceleration due to gravity, T_p is the peak period, and d_w is the depth of water. If the water depth is more than half the wavelength, the scour is likely to be negligible. If the water depth is less than one-half the wavelength, proceed to step 4.

4. Calculate the bottom orbital velocity (u_m) of the design wave: The bottom orbital velocity is the velocity at which the water particles move in a circular motion near the bottom due to the passage of the wave. This can be calculated using Equation 11 given as:

$$u_m = \frac{0.25}{(1 + At^2)^3} \times \frac{H_s}{T_n}$$

where $A = [6500 + (0.56 + 15.54t)^6]^{1/6}$, $t = T_n/T_z$, H_s is the significant wavelength, T_n is a natural scaling period $\left[= (d_w/g)^{1/2}\right]$, d_w is the depth of water, g is the acceleration due to gravity, T_z is the zero-crossing period $\left[= \left(T_p/1.281\right)\right]$, and T_p is the peak period.

5. Determine maximum scour depth (S_{max}) for the pier: The final step is to determine the maximum scour depth that is expected to occur due to the bottom orbital velocity. An expression (Equation 15) for the upper bound line of the plot given by Webb et al. (2014) is determined as shown in Figure 4. The maximum scour depth is the depth at which the foundation of the structure will be exposed, and it is important to ensure that the foundation is designed to withstand this depth of scour. Equation 15 (a and b) is used to calculate the maximum scour depth and represents the red line in Figure 3.

$$S_{max} = 0.14KC^{0.66} \times d_p \quad \text{when } KC < 30 \quad (15a)$$

$$S_{max} = d_p \quad \text{when } KC < 30 \quad (15b)$$

EXAMPLE CASES

To assess the practical effectiveness of the proposed methodology, we conducted a study using real-world data from three bridges located in Texas. Table 1 presents the specific input data used for each of the three bridges in the study. Additionally, we determined the 100-year wind speed for all three cases by analyzing historical wind data from the nearby Dallas Love Field airport

Table 1. Inputs data for different bridges.

Case	Lake Crossed	County	Lat	Lon	Depth of Water (m)	Diameter of Pier (m)
1	Lake Lavon	Collin	33.05287412	-96.42360119	4.3	0.61
2	Lake Ray Hubbard	Rockwall	32.92164297	-96.5055482	6.2	0.92
3	Lake Ray Hubbard	Rockwall	32.88864568	-96.49169114	9.0	0.76

To accurately determine the wind speed for our analysis, we assumed that the wind speeds were already measured at a height of 10 meters above ground level, so we did not need to make any adjustments for elevation. We utilized a probability distribution on a semi-log plot (Figure 5) to determine the 100-year wind speed. This technique involves plotting the natural logarithm of the wind speed values against the inverse of their cumulative probabilities. By using this method, we were able to account for the statistical distribution of wind speeds over time and accurately determine the 100-year wind speed for the analysis. After conducting this analysis, we determined that the 100-year wind speed was equal to 51.085 m/s for the three cases.

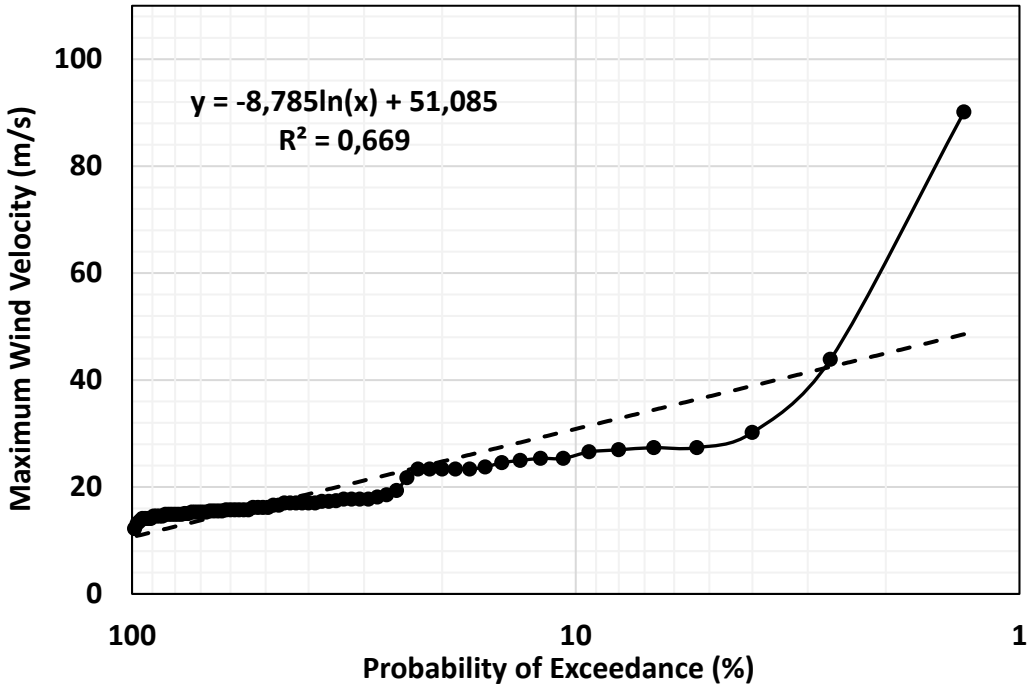

Figure 5. 100-year wind speed plot.

The significant wave height and peak period were calculated using the formula described in Step 2, and the bottom orbital velocity was calculated from Step 3. The resulting data including the input parameters and calculated scour depths, are presented in Table 2.

Table 2. Scour depths for different cases.

	Case 1	Case 2	Case 3
Depth of Water (m)	**4.30**	**6.20**	**9.00**
Diameter of Pier (m)	**0.61**	**0.92**	**0.76**
Fetch (m)	**3000**	**8000**	**8000**
Scour depth (m)	**0.172**	**0.286**	**0.246**

PARAMETRIC STUDY

To explore the impact of varying conditions on the proposed methodology, a parametric study was conducted. Specifically, we investigated the impact of four key parameters: the depth of water, the diameter of the pier, the fetch, and the 100-year wind speed. The results are as follows:

1. Depth of water: The water depth was varied from 1.5 m to 24 m in 5 increments and the corresponding scour depth was calculated for each level. Figure 6a shows the variation of scour depth with water depth shows that with an increase in the water depth, the scour depth decreases.

2. Diameter of the pier: The pier diameter was varied from 0.3 m to 3.6 m in 5 increments, and the scour depth was calculated for each diameter. Figure 6b shows that with an increase in pier diameter, the ratio between the scour depth and the pier diameter decrease.

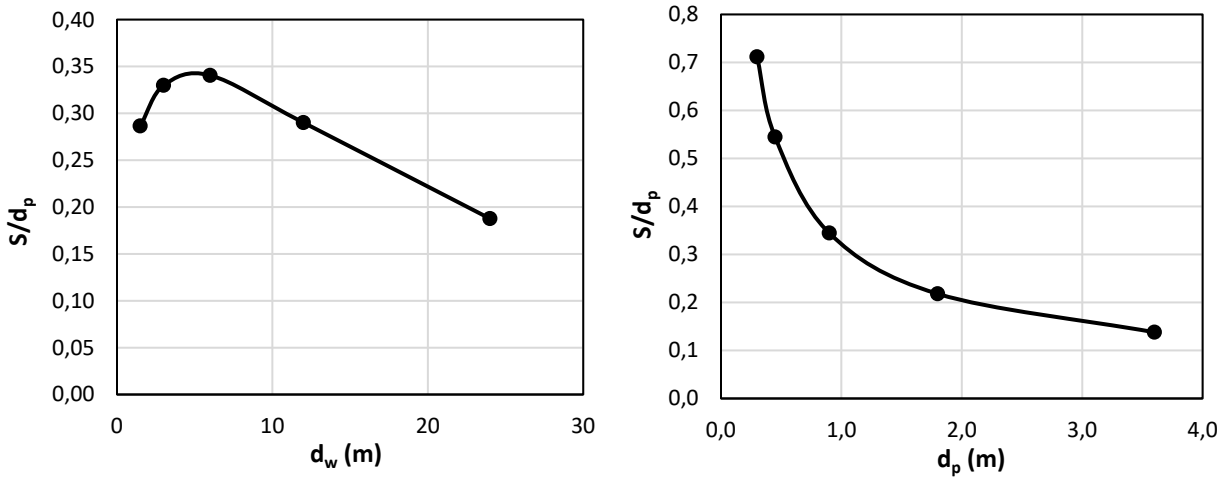

Figure 6. Variation in normalized scour depth for a) depth of water and b) diameter of the pier.

3. Fetch: The fetch was varied from 2500 m to 40000 m in 5 increments. Figure 7a shows that an increase in fetch results in an increase in scour depth.
4. 100-year wind speed: The 100-year wind speed was varied from 15 m/s to 240 m/s in 5 increments. As shown in Figure 7b, an increase in design wind speed leads to an increase in scour depth.

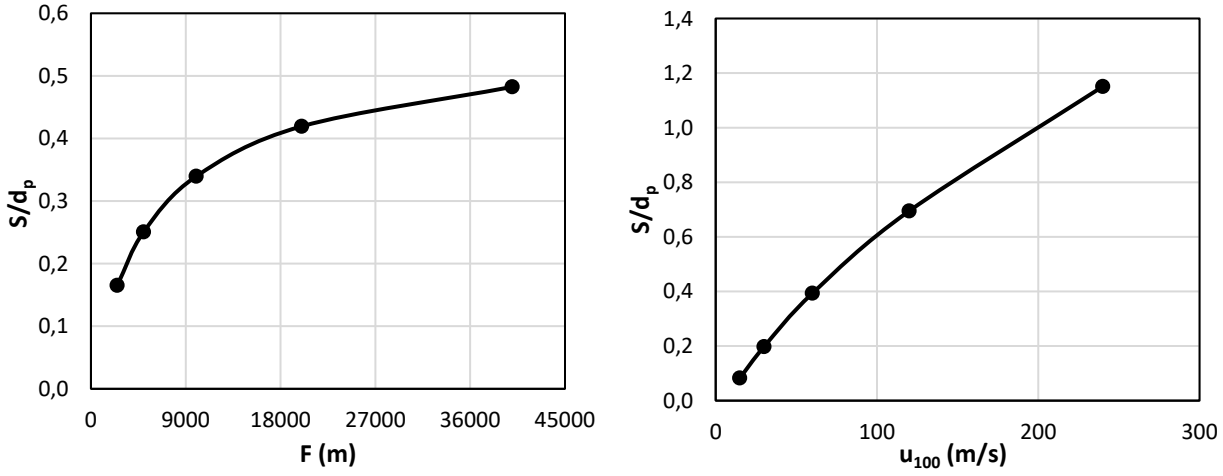

Figure 7. Variation in normalized scour depth for a) fetch and b) 100-year wind speed.

CONCLUSIONS

A step-by-step methodology for calculating the depth of wave related scour at bridge piers in lakes is presented. The input parameters are wind speed, water depth, fetch, and pier diameter. The steps are:

1. Select the design wind speed (U_w).
2. Determine significant wave height (H_s) and peak period (T_p) of the design wave.
3. Check water depth against wavelength.
4. Calculate the bottom orbital velocity (u_m) of the design wave.
5. Determine maximum scour depth (S_{max}) for the pier.

A parametric study is conducted to investigate the effects of these parameters on the scour depth. The most influential parameters in order of impact are wind speed, the diameter of the pier, depth of water, and fetch. The trends are as follows:

1. Depth of water: When the depth of water increases, the scour depth decreases.
2. Diameter of the pier: When the diameter of the pier increases, the scour depth increases.
3. Fetch: When the fetch increases, the scour depth increases.
4. 100-year wind speed: When the design speed increases, the scour depth increases.

Overall, the scour depth due to waves in lakes is very small when the water depth is more than one-half the wavelength; this is the case with deep waves. For shallow waves, the scour depth is rarely larger than one-half the pier diameter.

ACKNOWLEDGMENTS

The authors would like to acknowledge the support and assistance of the Texas Department of Transportation (TxDOT) in the research presented in this paper. We are grateful to them for their contributions to the data collection. TxDOT funded this work through Research and Technology Implementation Project Agreement. The opinions, findings, and conclusions are those of the authors and do not necessarily reflect the views of TxDOT.

REFERENCES

Booij, N. R., C., R., & L., H. H. (1999). "A third-generation wave model for coastal regions: Part 1. Model description and validation". *J. Geophysical Res.*, 7649-7666.

Briaud J.-L., Ali T., Chen H.C., (2023). "Synthesis of Lacustrine Wave Scour Evaluation Methods". *Texas A&M Transportation Institute*, Report 0-7163 to the Texas Dpt. of Transportation.

Chen, Q. L., Wang, H. Z., & S., L. D. (2007). "Prediction of storm surges and wind waves on coastal highways in hurricane-prone areas". *J. Coastal Res.*, 1304-1317.

Dey, S., Sumer, B. M. and Fredsøe, J. (2006). "Control of Scour at Vertical Circular Piles". 132(3), pp. 270–279. doi: 10.1061/(ASCE)0733-9429(2006)132.

Douglass, S. L., & J, Krolak. (2008). *Hydraulic Engineering Circular 25*. Highways in the Coastal Environment, 2nd ed. FHWA, U.S. Department of Transportation.

Gazi, A. H., Afzal, M. S. and Dey, S. (2019). "Scour around piers underwaves: Current status of research and its future prospect". *Water (Switzerland)*, pp. 1–14. doi: 10.3390/w11112212.

Hasselmann, K. B. (1973). "Measurements of wind-wave growth and swell decay during the Joint North Sea Wave Project (JONSWAP)". *Deutsche Hydrographisches Institut*, Hamburg, Suppl., A 8(12), 95.

Hughes, S. A. (1993). "Physical Models and Laboratory Techniques in Coastal Engineering". Hackensack, N.J.: *World Scientific.*

Lin, P. C., D. J. Schwab, & R. E. Jensen. (2002). "Has wind-wave modeling reached its limits?" *Ocean Engineering* 29(1), 81-89.

Longuet-Higgins, M. S. (1969). "A non-linear mechanism for the generation of sea waves". *Proc. Royal Soc. London A, 311*(1506), 371-389.

Madsen, O. (1994). "Spectral wave-current bottom boundary layer flows". *Coastal Engineering 1994: Proceedings*, 24th International Conference, Coastal Engineering Research Council (pp. 384–398). Kobe, Japan: American Society of Civil Engineers.

Miles, J. W. (1957). "On the generation of surface waves by shear flows". *Journal of Fluid Mechanics*, 3, 185-204.

Olsen, N. R. B. (2002). "Hydro informatics, fluvial hydraulics and limnology". *Norwegian University of Science and Technology*. Trondheim, Noruega. Available at: http://folk.ntnu.no/nruther/TVM4155/flures5.pdf.

Phillips, O. M. (1957). "On the generation of waves by turbulent winds". *Journal Fluid Mechanics*, 2, 217-445.

Ris, R. C., L. H. Holthuijsen, and N. Booij. (1999). "A third-generation wave model for coastal regions: Part 2. Model description and validation". *J. Geophysical Res*. 104(C4): 7667 - 7681.

Sorensen, R. M. (1993). *Basic Wave Mechanics for Coastal and Ocean Engineers.* New York, N.Y.: John Wiley and Sons.

Soulsby, R. (1987). "Calculating bottom orbital velocity beneath waves". *Coastal Engineering*, 371-380.

SPM. (1973). *Shore Protection Manual*. U.S Army Coastal Engneering Research Center: Washington, D.C, Vol. 2.

SPM. (1984). *Shore Protection manual.* U.S. Army Engineer Waterways Experiment Station: Vol 2, 4th ed, Washington, D.C.

Sumer, B. M., Hatipoglu, F. and Fredsøe, J. (2007). "Wave Scour around a Pile in Sand, Medium Dense". *J. Waterw. Port Coast. Ocean Eng*., 133, 14-27. doi: 10.1061/(ASCE)0733-950X(2007)133.

Sumer, B. M., & Fredsøe, J. (1998). "Wave Scour Around Group of Vertical Piles". *Journal of Waterway, Port, Coastal, and Ocean Engineering,* 248-256.

Sumer, B., & Fredsøe, J. (2001). "Scour around pile in combined waves and current". *J. Hydraul. Eng.*, 403-411.

Sumer, B., Fredsøe, J., & Christiansen, N. (1992). "Scour around vertical pile in waves". *J.Waterw. Port Coast. Ocean Eng*., 15-31.

Vincent, C. L., Z. Demirbilek, & J. R. Weggel. (2002). "Estimation of nearshore waves". Chapter II in *Coastal Engineering Manual: Part II. Coastal Hydrodynamics. Engineering Manual* 1110-2-1100. L. Vincent and Z. Demirbilek, eds. Washington, D.C, U.S: Army Corps of Engineers.

Webb, B. M., & Matthews, M. T. (2014). "Wave-Induced Scour at Cylindrical Piles Estimating Equilibrium Scour Depth in a Transition Zone". *Journal of the Transportation Research Board,* 148-155.

Young, I. R., & Verhagen, L. A. (1996). "The growth of fetch limited waves in water of finite depth 1. Total energy and peak frequency". *Coastal Engineering,* 29, 47-78.